

## Substrate Binding Favors Enhanced NO Binding to P450<sub>cam</sub>

Alicja Franke,<sup>†,‡</sup> Grazyna Stochel,<sup>‡</sup> Christiane Jung,<sup>§</sup> and Rudi van Eldik<sup>\*,†</sup>

Contribution from the Institute for Inorganic Chemistry, University of Erlangen-Nürnberg, Egerlandstr. 1, 91058 Erlangen, Germany, Department of Inorganic Chemistry, Jagiellonian University, Ingardena 3, 30 060 Kraków, Poland, and Max Delbrück Center for Molecular Medicine, Robert Rössle Strasse 10, D-13125 Berlin-Buch, Germany

Received September 29, 2003; E-mail: vaneldik@chemie.uni-erlangen.de

**Abstract:** Ferric cytochrome P450<sub>cam</sub> from *Pseudomonas putida* (P450<sub>cam</sub>) in buffer solution at physiological pH 7.4 reversibly binds NO to yield the nitrosyl complex P450<sub>cam</sub>(NO). The presence of 1*R*-camphor affects the dynamics of NO binding to P450<sub>cam</sub> and enhances the association and dissociation rate constants significantly. In the case of the substrate-free form of P450<sub>cam</sub>, subconformers are evident and the NO binding kinetics are much slower than in the presence of the substrate. The association and dissociation processes were investigated by both laser flash photolysis and stopped-flow techniques at ambient and high pressure. Large and positive values of  $\Delta S^\ddagger$  and  $\Delta V^\ddagger$  observed for NO binding to and release from the substrate-free P450<sub>cam</sub> complex are consistent with the operation of a limiting dissociative ligand substitution mechanism, where the lability of coordinated water dominates the reactivity of the iron(III)-heme center with NO. In contrast, NO binding to P450<sub>cam</sub> in the presence of camphor displays negative activation entropy and activation volume values that support a mechanism dominated by a bond formation process. Volume profiles for the binding of NO appear to be a valuable approach to explain the differences observed for P450<sub>cam</sub> in the absence and presence of the substrate and enable the clarification of the underlying reaction mechanisms at a molecular level. Changes in spin state of the iron center during the binding/release of NO contribute significantly to the observed volume effects. The results are discussed in terms of relevance for the biological function of cytochrome P450 and in context to other investigations of the related reactions between NO and imidazole- and thiolate-ligated iron(III) hemoproteins.

### Introduction

Cytochrome P450 enzymes are a widely distributed family of b-type hemoproteins involved in a diversity of vital processes, such as the biosynthesis of lipids and steroids, degradation of xenobiotics, drug metabolism, and carcinogenesis.<sup>1,2</sup> They catalyze the oxidation of a variety of hydrophobic compounds using a common reaction mechanism that involves the heterolytic O—O bond cleavage of the heme-bound O<sub>2</sub> and subsequent formation of the putative active species (compound I).<sup>1,3</sup>

It was shown that small molecules are able to bind to the heme iron of P450 and may be used as a sensitive probe of the heme region to get new insights into P450 structure—function relationships. Unlike CO, nitric oxide can bind to both ferric and ferrous forms of cytochrome P450,<sup>4</sup> the latter one forming iron-nitrosyl complexes that are in their electronic structure and geometry similar to the physiologically important dioxygen

complexes of cytochrome P450. Furthermore, several lines of evidence<sup>5</sup> indicate that P450 enzymes might be primary targets for the nitric oxide action in vivo. Nitric oxide readily reacts with microsomal P450s that metabolize various compounds, including steroids and eicosanoids.<sup>6</sup> This interaction can proceed in two different ways: (1) NO reversibly binds to the heme moiety forming an iron-nitrosyl complex (reversible inhibition characterized by complete cessation of the catalytic activity) or it can irreversibly inactivate microsomal P450 through modification of their cysteinyl residues (formation of nitrosyl-thiols).<sup>7</sup>

Among various cytochromes P450, cytochrome P450<sub>cam</sub> in its substrate-free or substrate-bound form has been most thoroughly characterized<sup>8,9</sup> and is now considered the best model system for understanding the reaction mechanism by which small molecules such as CO, O<sub>2</sub>, or NO undergo coordination

<sup>†</sup> University of Erlangen-Nürnberg.

<sup>‡</sup> Jagiellonian University.

<sup>§</sup> Max Delbrück Center for Molecular Medicine.

- (1) Sono, M.; Roach, M. P.; Coulter, E. D.; Dawson, J. H. *Chem. Rev.* **1996**, *96*, 2841 and references therein.
- (2) (a) Wislocki, P. G.; Lu, A. Y. H. Reactions catalysed by the cytochrome P-450 system. In *Enzymatic Basis of Detoxication*; Jacoby WB, Ed.; Academic Press: New York, 1980; Vol. 1, pp 135–182. (b) Guengerich F. P. *J. Biol. Chem.* **1991**, *266*, 10019.
- (3) Dawson, J. H.; Sono, M. *Chem. Rev.* **1987**, *87*, 1255 and references therein.
- (4) (a) Ebel, R. E.; O'Keefe, D. H.; Peterson, J. A. *FEBS Lett.* **1975**, *55* (1), 198. (b) O'Keefe, D. H.; Ebel, R. E.; Peterson, J. A. *J. Biol. Chem.* **1978**, *253* (10), 3509.

- (5) (a) Hanke, C. J.; Drewett, J. G.; Myers, C. R.; Campbell, W. B. *Endocrinology* **1998**, *139*, 4053. (b) del Punta, K.; Charreau, E. H.; Pignataro, O. *Endocrinology* **1996**, *137*, 5337.
- (6) (a) Takemura, S.; Minamiyama, Y.; Imaoka, S.; Funae, Y.; Hirohashi, K.; Inoue, M.; Kinoshita, H. *J. Hepatology* **1999**, *30*, 1035. (b) Wink, D. A.; Osawa, Y.; Darbyshire, J. F.; Jones, C. R.; Eshenaur, S. C.; Nims, R. W. *Arch. Biochem. Biophys.* **1993**, *300* (1), 115.
- (7) Minamiyama, Y.; Takemura, S.; Imaoka, S.; Funae, Y.; Tanimoto, Y.; Inoue, M. *J. Pharmacol. Exp. Ther.* **1997**, *283*, 1479.
- (8) Murray, R. I.; Fisher, M. T.; Debrunner, G.; Sligar, S. G. In *Metalloproteins Part I: Metal Proteins with Redox Roles*; Harrison, P. M., Ed.; Verlag Chemie: Weinheim, 1985; pp 157.
- (9) Dawson, J. H.; Eble, K. S. *Adv. Inorg. Bioinorg. Mech.* **1986**, *4*, 1.

to the heme iron center of many biomolecules. Cytochrome P450<sub>cam</sub> isolated from the bacterium *Pseudomonas putida* catalyses the regio- and stereospecific hydroxylation of camphor to the 5-exo alcohol<sup>10</sup> and like other P450s utilizes the thiolate as the proximal ligand of the heme iron atom.<sup>11</sup> X-ray crystallographic studies<sup>12</sup> clearly showed that the active site of P450<sub>cam</sub> is extremely hydrophobic and deeply buried inside the enzyme with the substrate binding site lying in close proximity of the heme moiety. The binding of camphor to the resting form of P450<sub>cam</sub> causes changes in the heme environment and its electronic structure.<sup>13</sup> The substrate-free ferric P450<sub>cam</sub> is a low-spin ( $S = 1/2$ ), six-coordinate complex with a water cluster bound at the distal site *trans* to the cysteine axial ligand in the proximal position. Upon binding of camphor to the active site, the water molecules are expelled from the coordination sphere to form a high-spin ( $S = 5/2$ ) pentacoordinate iron heme center.

When NO reacts with the ferric form of P450<sub>cam</sub> (in the absence and in the presence of camphor) a diamagnetic (EPR silent), six-coordinate complex is produced.<sup>4</sup> The nitrosyl complex of P450<sub>cam</sub> is relatively stable at 5 °C in the absence of oxygen and, in contrast to NO complexes of other ferric hemoproteins (e.g., methemoglobin or metmyoglobin), does not undergo subsequent reductive nitrosylation.<sup>4</sup> A Resonance Raman study<sup>14</sup> on the NO adduct of cytochrome P450<sub>cam</sub>, formally described as Fe<sup>II</sup>-NO<sup>+</sup>, revealed that the Fe-NO group adopts a linear structure in the absence of camphor but becomes slightly bent upon binding of the substrate. Computational studies<sup>15</sup> on the interaction between NO and the active site of ferric cytochrome P450 (DFT and SAM1 semiempirical methods) have assessed the feasibility of the displacement of a water molecule by NO as the first step in the reversible inhibition of cytochrome P450. However, the possibility of an alternative mechanism involving attack of NO on the sulfur of the cysteine has not been excluded and modeling of this reaction pathway is the subject of further studies.

To further elucidate the mechanism of action of cytochrome P450 and to understand the essence of its biological functions, it is necessary to gain detailed insight into ligand or substrate binding to the catalytic site of the enzyme. Whereas the reactions of ferrous cytochrome P450 with carbon monoxide have already been extensively investigated with the application of several kinetic methods<sup>16</sup> and under various conditions<sup>17</sup> (high pressure,

low temperature, and for different mutations), fewer kinetic studies have been carried out on the binding of NO to ferric/ferrous P450.<sup>18–20</sup> We have, therefore, in the present study focused our attention on the kinetics and mechanistic interpretation of the reversible binding of NO to P450<sub>cam</sub> in the absence and presence of substrate molecules (1*R*-camphor). Temperature and pressure effects on the reaction rates probed by stopped-flow and laser flash photolysis experiments at ambient and elevated pressure enable the extraction of appropriate rate and activation parameters ( $\Delta G^\ddagger$ ,  $\Delta H^\ddagger$ ,  $\Delta S^\ddagger$ , and  $\Delta V^\ddagger$ ) for the studied reactions and allow us to gain insight into the details of the underlying reaction mechanisms. On the basis of the activation volumes for the reversible binding of NO, volume profiles for the binding of NO to the free and camphor-bound forms of cytochrome P450<sub>cam</sub> could be constructed for the first time. This enables us to discuss the apparent difference observed for the binding mechanism of NO in the absence and presence of the substrate in relevance to the biological function of cytochrome P450. Furthermore, a comparison with the results obtained earlier in our laboratories for the related reaction between NO and the imidazole-ligated hemoprotein, metmyoglobin, could be made.<sup>21</sup>

## Experimental Section

**Materials.** All solutions were prepared with deionized (Millipore) water. Cytochrome P450<sub>cam</sub> expressed in *Escherichia coli* strain TB1 was isolated and purified according to Jung et al.<sup>17f</sup> The natural substrate 1*R*-camphor was removed by dialysis and column chromatography to obtain the substrate-free protein.<sup>17f</sup> The substrate 1*R*-camphor (98%) was purchased from Aldrich. Glycerol (spectrophotometric grade, 99.5%) was obtained from Acros Organics. Na[Ru<sup>III</sup>(Hedta)Cl] was prepared according to the method of Diamantis and Dubrawski,<sup>22</sup> and its purity was checked by elemental analysis and UV–vis spectroscopy. All other chemicals used throughout this study were of analytical reagent grade.

NO gas, purchased from Riessner Gase or Linde 93 in a purity of at least 99.5 vol %, was cleaned of trace quantities of higher nitrogen oxides such as N<sub>2</sub>O<sub>3</sub> and NO<sub>2</sub> by passing it through an Ascarite II column (NaOH on silica gel, Sigma-Aldrich) and then bubbling through a gas scrubbing bottle containing 5 M NaOH (Aldrich).

**Solution Preparation.** All solutions were prepared under strict exclusion of air oxygen. Solutions were prepared using 0.1 M potassium phosphate buffer (Merck), pH = 7.4 (at 25 °C) with 20% (w/w) glycerol. Glycerol was added to prevent cytochrome P420 formation, as was shown for different glycerol contents by Jung et al.<sup>17c</sup> In the case of experiments with the camphor-bound form of cytochrome P450<sub>cam</sub>, a saturated

- (10) (a) Dawson, J. H.; Sono, M. *Chem. Rev.* **1987**, *87*, 1255. (b) Mueller, E. J.; Loida, P. J.; Sligar, S. G. In *Cytochrome P450: Structure, Mechanism, and Biochemistry*, 2nd ed.; Ortiz de Montellano, P. R. Ed.; Plenum: New York, 1995; Chapter 3, pp 83–124.
- (11) (a) Auclair, K.; Moëne-Loccoz, P.; Ortiz de Montellano, P. R. *J. Am. Chem. Soc.* **2001**, *123*, 4877. (b) Sono, M.; Dawson, J. H. *J. Biol. Chem.* **1982**, *257*, 5496. (c) Sono, M.; Andersson, L. A.; Dawson, J. H. *J. Biol. Chem.* **1982**, *257*, 8308.
- (12) (a) Poulos, T. L.; Finzel, B. C.; Howard, A. J. *Biochemistry* **1986**, *25*, 5314. (b) Poulos, T. L.; Finzel, B. C.; Gunsalus, I. C.; Wagner, G. C.; Kraut, J. *J. Biol. Chem.* **1985**, *260*, 16122.
- (13) (a) Raag, R.; Poulos, T. L. *Biochemistry* **1989**, *28*, 917. (b) Sligar, S. G. *Biochemistry* **1976**, *15*, 5399.
- (14) Hu, S.; Kincaid, J. R. *J. Am. Chem. Soc.* **1991**, *113*, 2843.
- (15) Scherlis, D. A.; Cymeryng, C. B.; Estrin, D. A. *Inorg. Chem.* **2000**, *39*, 2352.
- (16) (a) Kato, M.; Makino, R.; Iizuka, T. *Biochim. Biophys. Acta* **1995**, *1246*, 178. (b) Unno, M.; Ishimori, K.; Ishimura, Y.; Morishima, I. *Biochemistry* **1994**, *33*, 9762. (c) Koley, A. P.; Robinson, R. C.; Friedmann, F. K. *Biochimie* **1996**, *78*, 706.
- (17) (a) Jung, C.; Bec, N.; Lange, R. *Eur. J. Biochem.* **2002**, *269*, 2989. (b) Jung, C. *Biochim. Biophys. Acta* **2002**, *1595*, 309. (c) Jung, C.; Huo Bon Hoa, G.; Davydow, D.; Gill, E.; Heremans, K. *Eur. J. Biochem.* **1995**, *233*, 600. (d) Schulze, H.; Hui Bon Hoa, Jung, C. *Biochim. Biophys. Acta* **1997**, *1338*, 77. (e) Schulze, H.; Ristau, O.; Jung, C. *Biochim. Biophys. Acta* **1994**, *1183*, 491. (f) Jung, C.; Hui Bon Hoa, G.; Schöder, K.-L.; Simon, M.; Doucet, J. P. *Biochemistry* **1992**, *31*, 12855.

- (18) Nakano, R.; Sato, H.; Watanabe, A.; Ito, O.; Shimizu, T. *J. Biol. Chem.* **1996**, *271* (15), 8570.
- (19) (a) Shiro, Y.; Fujii, M.; Iizuka, T.; Adachi, S.; Tsukamoto, K.; Nakahara, K.; Shoun, H. *J. Biol. Chem.* **1995**, *270* (4), 1617. (b) Obayashi, E.; Tsukamoto, K.; Adachi, S.; Takahashi, S.; Nomura, M.; Iizuka, T.; Shoun, H.; Shiro, Y. *J. Am. Chem. Soc.* **1997**, *119*, 7807.
- (20) (a) Scheele, J. S.; Bruner, E.; Kharitonov, V. G.; Martásek, P.; Roman, L. J.; Masters, B. S. S.; Sharma, V. S.; Magde, D. *J. Biol. Chem.* **1999**, *274* (19), 13105. (b) Abu-Soud, H. M.; Wang, J.; Rousseaus, D.; Fukuto, J. M.; Ignarro, L. J.; Stuehr, D. J. *Biol. Chem.* **1995**, *270* (39), 22997. (c) Abu-Soud, H. M.; Ichimoris, K.; Presta, A.; Stuehr, D. J. *J. Biol. Chem.* **2000**, *275* (23), 17349. (d) Huang, L.; Abu-Soud, H. M.; Hille, R.; Stuehr, D. J. *Biochemistry*, **1999**, *38*, 1912.
- (21) Laverman, L. E.; Wanat, A.; Oszejca, J.; Stochel, G.; Ford, P. C.; van Eldik, R. J. *Am. Chem. Soc.* **2001**, *123*, 285.
- (22) Diamantis, A. A.; Dubrawski, J. V. *Inorg. Chem.* **1981**, *20*, 1142.

aqueous camphor solution was added to the buffered glycerol mixture to a final camphor concentration of 0.5 mM. Buffer solutions were carefully deoxygenated for extended periods with pure N<sub>2</sub> or Ar before they were brought in contact with aliquots of the P450<sub>cam</sub> stock solution. Concentrations of the substrate-free and camphor-bound forms of P450<sub>cam</sub> were determined spectrophotometrically at 417 nm ( $\epsilon = 115 \text{ mM}^{-1} \text{ cm}^{-1}$ ) and 391 nm ( $\epsilon = 102 \text{ mM}^{-1} \text{ cm}^{-1}$ ), respectively.

A stock solution of NO was prepared by degassing a buffer solution, followed by saturation with NO to a final concentration of 0.0019 M at 25 °C. Dilutions of known concentration were prepared from this saturated solution by the use of a syringe technique.

**Measurements.** pH measurements were performed on a Metrohm 623 pH meter equipped with a Sigma glass electrode. The concentration of free NO in buffered solution was determined with an ISO-NOP electrode connected to an ISO-NO Mark II nitric oxide sensor from World Precision Instruments.<sup>23</sup> The NO electrode was calibrated daily with fresh solutions of sodium nitrite and potassium iodide according to the method suggested by the manufacturers. The calibration factor nA/ $\mu\text{M}$  was determined with a linear fit program. UV-vis spectra were recorded in gastight cuvettes on a Shimadzu UV-2100 spectrophotometer equipped with a thermostated cell compartment CPS-260.

**Kinetic Measurements. Laser Flash Photolysis at Ambient and High Pressure.** Laser flash photolysis kinetic studies were carried out with the use of the LKS.60 spectrometer from Applied Photophysics for detection and a Nd:YAG laser (SURLITE I-10 Continuum) pump source operating in the second ( $\lambda_{\text{exc}} = 532 \text{ nm}$ ) harmonics (245 mJ pulses with  $\sim 7 \text{ ns}$  pulse widths). Spectral changes at appropriate wavelengths were monitored using a 100-W xenon arc lamp, monochromator, and photomultiplier tube PMT-1P22. The absorbance reading was balanced to zero before the flash, and data were recorded on a digital storage oscilloscope DSO HP 54522A and then transferred to a PC for subsequent analysis. The rate constants were detected at 431 nm, where a maximum in the UV-vis spectrum for P450<sub>cam</sub>-NO complex is observed. Gastight quartz cuvettes and a pill-box cell combined with a high-pressure system<sup>24</sup> were used at ambient and high pressure (up to 130 MPa), respectively. At least 20 kinetic runs were recorded under all conditions, and the reported rate constants represent the mean value of these. For time-resolved optical (TRO) absorption measurements, a photomultiplier tube (PMT) detector was employed to obtain kinetic traces at a single observation wavelength. TRO spectra were recorded point by point by using a monochromator in the optical train to vary the observation wavelength.

**Stopped-Flow Kinetics.** Stopped-flow studies on the reaction of NO with P450<sub>cam</sub> were carried out using an SX-18MV (Applied Photophysics) stopped-flow spectrometer. Deoxygenated buffered solutions of P450<sub>cam</sub> were rapidly mixed with buffered solutions with various [NO], and the changes in absorbance at 417 or 431 nm were monitored. Dissociation rate constants for the nitrosyl complex of P450<sub>cam</sub> were studied by rapidly mixing a P450<sub>cam</sub>-NO complex solution (containing a

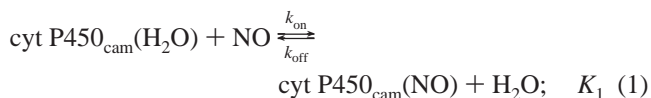
slight excess of NO) with an excess of [Ru(edta)H<sub>2</sub>O]<sup>-</sup>, formed instantaneously on dissolution of Na[Ru(Hedta)Cl] in aqueous solution.

**High-Pressure Stopped-Flow.** High-pressure stopped-flow experiments were performed on a custom-built instrument described previously<sup>25,26</sup> at pressures up to 130 MPa. Kinetic traces were recorded at 417 or 431 nm on an IBM-compatible PC and analyzed with the OLIS KINFIT (Bogart, GA, 1989) set of programs.

All kinetic experiments were performed under pseudo-first-order conditions, i.e., with at least a 10-fold excess of NO. The studied reactions exhibited pseudo-first-order behavior for at least three half-lives. In all stopped-flow experiments, at least five kinetic runs were recorded under all conditions, and the reported rate constants represent the mean values.

## Results

**UV-vis Observations and Kinetics of the Binding of NO to Substrate-Free Cytochrome P450<sub>cam</sub>.** The oxidized substrate-free form of P450<sub>cam</sub> is almost 100% in the low-spin state at room temperature and atmospheric pressure and exhibits in 0.1 M potassium phosphate buffer (pH = 7.4) a Soret band maximum at 417 nm ( $\epsilon = 115 \text{ mM}^{-1} \text{ cm}^{-1}$ ) and  $\alpha$  and  $\beta$  bands at 569 (11.1  $\text{mM}^{-1} \text{ cm}^{-1}$ ) and 536 nm (10.6  $\text{mM}^{-1} \text{ cm}^{-1}$ ), respectively. Addition of NO to the degassed solution of substrate-free P450<sub>cam</sub> led to the formation of a single, spectrally distinct species with a Soret maximum at 432.5 nm (103  $\text{mM}^{-1} \text{ cm}^{-1}$ ) and visible bands at 541 (15  $\text{mM}^{-1} \text{ cm}^{-1}$ ) and 571 nm (12.3  $\text{mM}^{-1} \text{ cm}^{-1}$ ). The uptake of NO appears to be completely reversible as judged from experiments in which a stream of Ar gas was used to remove NO from the nitrosyl complex solution (Figure 1a), consistent with the equilibrium described by eq 1. Since only one of the water molecules in the [H<sub>2</sub>O]<sub>6</sub> cluster is directly bound to the iron(III) center, in all equations and schemes shown in this paper substrate-free cytochrome P450<sub>cam</sub> is presented as cyt P450<sub>cam</sub>(H<sub>2</sub>O).



Spectral changes coupled to the detection of free NO in solution using the NO electrode enabled the determination of the equilibrium constant for reaction 1. The  $K_1$  value was calculated to be  $(9.0 \pm 0.2) \times 10^5 \text{ M}^{-1}$  at 25 °C in 0.1 M phosphate buffer and is in good agreement with the ratios of the “on” and “off” rate constants ( $K_1 = k_{\text{on}}/k_{\text{off}}$ ) determined under similar conditions (see below). The rate of reaction 1 with NO in large excess is expected to follow pseudo-first-order kinetics for which the observed rate constant,  $k_{\text{obs}}$ , can be expressed by eq 2:

$$k_{\text{obs}} = k_{\text{on}}[\text{NO}] + k_{\text{off}} \quad (2)$$

The plot of  $k_{\text{obs}}$  vs [NO] should be linear with slope  $k_{\text{on}}$  and a nonzero intercept  $k_{\text{off}}$ . However, the value of the equilibrium constant  $K_1$  seems to be too high that extrapolation to [NO] = 0 does not allow an accurate determination of  $k_{\text{off}}$ . Therefore,

(23) Kudo, S.; Bourassa, J. S. E.; Sato, Y.; Ford, P. C. *Anal. Biochem.* **1997**, *247*, 193.

(24) Spitzer, M.; Gärtig, F.; van Eldik, R. *Rev. Sci. Instrum.* **1988**, *59*, 2092.

(25) van Eldik, R.; Palmer, D. A.; Schmidt, R.; Kelm, H. *Inorg. Chim. Acta* **1981**, *50*, 131.

(26) van Eldik, R.; Gaede, W.; Wieland, S.; Kraft, J.; Spitzer, M.; Palmer, D. A. *Rev. Sci. Instrum.* **1993**, *64*, 1355.

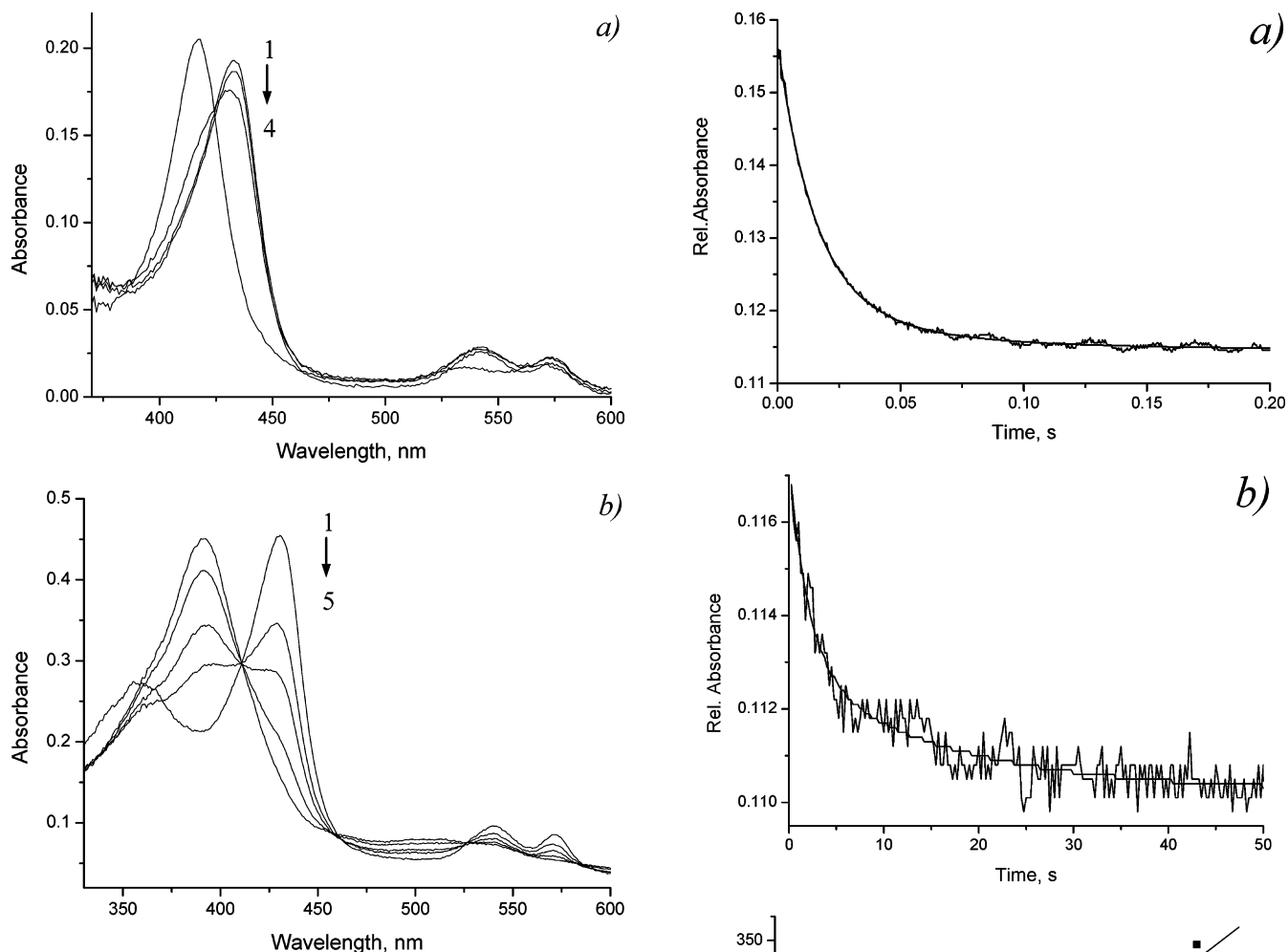


**Figure 1.** Absorption spectral changes recorded for the reaction of  $1.7 \times 10^{-6}$  M substrate-free (a) and  $4.4 \times 10^{-6}$  M camphor-bound (b) P450<sub>cam</sub> with NO in 0.1 M potassium phosphate buffer, pH = 7.4,  $T = 25$  °C. Curves: trace 1, P450<sub>cam</sub> saturated with NO; traces 2–4 (or 5 in the presence of camphor), P450<sub>cam</sub>(NO) following the bubbling of Ar through the solution for a short period.

the rate constants for the dissociation of NO from P450<sub>cam</sub>(NO) were determined in a more direct way, e.g., by using an NO-trapping technique<sup>27a</sup> combined with the stopped-flow method.

**Kinetics of the “On” Reaction.** The rates of NO binding to the substrate-free ferric form of cytochrome P450<sub>cam</sub> appear to be convenient to be measured by stopped-flow techniques. The typical absorbance–time trace obtained from the stopped-flow measurements at a single wavelength cannot be fitted satisfactorily with a single-exponential function and clearly shows the occurrence of two processes that differ significantly in their time scales. Kinetic traces recorded within 0.2 s at 25 °C (Figure 2a) represents absorbance changes at 417 nm that are *mainly* related to the faster reaction phase. A slight drift observed at the end of the kinetic trace clearly indicates occurrence of a second much slower reaction phase. As can be seen from the absorbance–time trace recorded on a much longer time scale (Figure 2b), the slow phase takes place within ca. 50 s at 25 °C and is accompanied by a much (almost 10 times) smaller absorbance change than those observed for the fast reaction

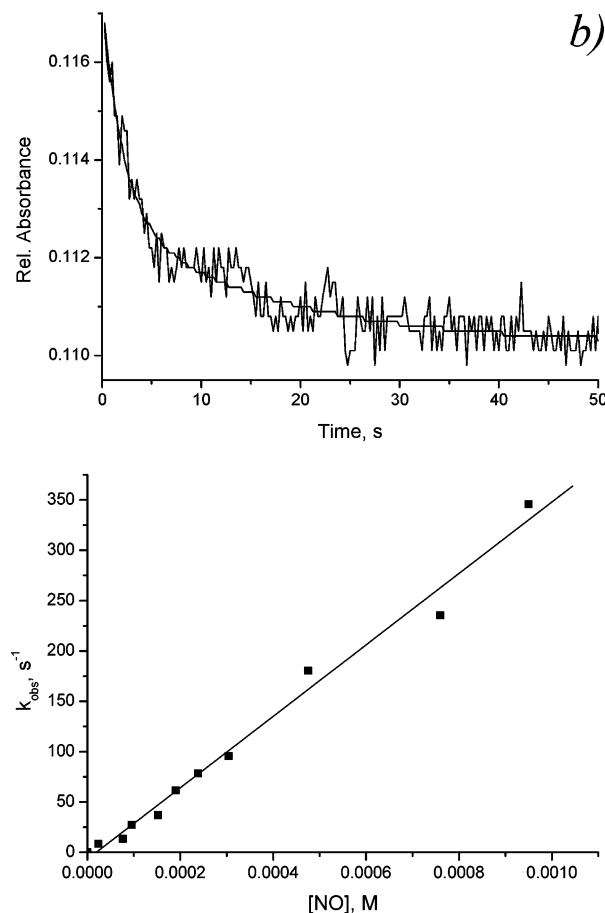


**Figure 2.** Plot of  $k_{\text{obs}}$  as a function of [NO] for the reaction of substrate-free P450<sub>cam</sub> with NO (fast reaction). Experimental conditions: [P450<sub>cam</sub>] =  $1.5 \times 10^{-6}$  M in 0.1 M potassium phosphate buffer, pH = 7.4,  $T = 25$  °C, detection at 417 nm. (a) and (b) Typical absorbance–time plots for the fast and slow reactions, respectively, recorded at 417 nm with the stopped-flow technique.

phase. Similar two-phase kinetics were observed before for CO binding to the ferrous form of cytochrome P450<sub>cam</sub> (substrate-free and camphane-bound form),<sup>17a,28</sup> cytochrome P450<sub>BM-3</sub><sup>29a</sup> and nitric oxide synthase.<sup>29b,c</sup>

(27) (a) Schnepfensieper, T.; Wanat, A.; Stochel, G.; Goldstein, S.; Meyerstein, D.; van Eldik, R. *Eur. J. Inorg. Chem.* **2001**, 2317. (b) Davies, N. A.; Wilson, M. T.; Slade, E.; Fricker, S. P.; Murrer, B. A.; Powell, N. A.; Henderson, G. R. *Chem. Commun.* **1997**, 47.

(28) Unno, M.; Ishimori, K.; Ishimura, Y.; Morishima, I. *Biochemistry* **1994**, *33*, 9762.

(29) (a) McLean, M. A.; Yeom, H.; Sligar, S. G. *Biochimie* **1996**, *78*, 700. (b) Scheele, J. S.; Kharitonov, V. G.; Martásek, P.; Roman, L. J.; Sharma, V. S.; Masters, B. S. S.; Magde, D. *J. Biol. Chem.* **1997**, *272*, 12523. (c) Matsuoka, A.; Stuehr, D. J.; Olson, J. S.; Clark, P.; Ikeda-Saito, M. *J. Biol. Chem.* **1994**, *269*, 20335.

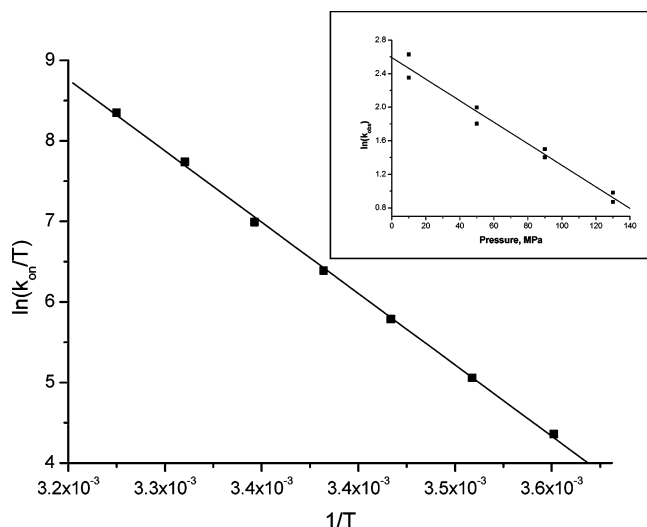


**Figure 3.** Eyring plot of  $\ln(k_{\text{on}}/T)$  vs  $1/T$  for NO binding to substrate-free P450<sub>cam</sub> (fast reaction). Experimental conditions:  $[\text{P450}_{\text{cam}}] = 1.5 \times 10^{-6}$  M,  $[\text{NO}] = 1.9 \times 10^{-4}$  M in 0.1 M potassium phosphate buffer, pH = 7.4,  $\lambda_{\text{det}} = 417$  nm. Inset:  $k_{\text{obs}}$  as a function of pressure measured for the reaction at 5 °C,  $[\text{P450}_{\text{cam}}] = 2.4 \times 10^{-6}$  M and  $[\text{NO}] = 4.75 \times 10^{-4}$  M in 0.1 M potassium phosphate buffer, pH = 7.4, 20% glycerol.

**Table 1.** Rate Constants and Activation Parameters for “On” and “Off” Reactions for NO Binding to Substrate-Free Cytochrome P450<sub>cam</sub>

T/°C	P/MPa	“on” reaction		“off” reaction
		$k_{\text{on}}$ (fast phase) ( $\times 10^{-4}$ ) M <sup>-1</sup> s <sup>-1</sup>	$k_{\text{on}}$ (slow phase) ( $\times 10^{-3}$ ) M <sup>-1</sup> s <sup>-1</sup>	$k_{\text{off}}$ s <sup>-1</sup>
5.0	0.1	2.2 ± 0.2		
10.0		4.5 ± 0.3	0.6 ± 0.1	0.026 ± 0.003
15.0		9.4 ± 0.3	1.5 ± 0.3	
17.5				0.10 ± 0.01
20.0		17.4 ± 0.3	3.2 ± 0.5	
25.0		32.4 ± 0.2	5.8 ± 0.7	0.35 ± 0.02
30.0		70 ± 3	10 ± 1	
35.0		131 ± 10	16 ± 2	2.0 ± 0.4
5.0	10	2.2 ± 0.1	0.9 ± 0.2	
	50	1.4 ± 0.1	0.44 ± 0.08	
	90	0.9 ± 0.1	0.28 ± 0.04	
	130	0.54 ± 0.04	0.19 ± 0.03	
20.0	10			0.14 ± 0.01
	50			0.066 ± 0.006
	90			0.037 ± 0.002
	130			0.022 ± 0.004
$\Delta H^{\ddagger}$ kJ mol <sup>-1</sup>		92 ± 1	90 ± 4	122 ± 4
$\Delta S^{\ddagger}$ J mol <sup>-1</sup> K <sup>-1</sup>		+169 ± 4	+128 ± 15	+155 ± 15
$\Delta V^{\ddagger}$ cm <sup>3</sup> mol <sup>-1</sup>		+28 ± 2	+30 ± 3	+31 ± 1

In agreement with eq 2, plots of  $k_{\text{obs}}$  vs  $[\text{NO}]$  for the fast and slow phase of the binding of NO to substrate-free P450<sub>cam</sub> were found to be linear with almost zero intercepts. A typical NO concentration dependence at 25 °C for the fast phase is shown in Figure 2. The binding rate constant for the faster phase,  $k_{\text{on}}^{\text{(fast)}} = (3.2 \pm 0.1) \times 10^5$  M<sup>-1</sup> s<sup>-1</sup>, appears to be 55 times faster than that for the slower phase,  $k_{\text{on}}^{\text{(slow)}} = (5.8 \pm 0.1) \times 10^3$  M<sup>-1</sup> s<sup>-1</sup> at 25 °C in 0.1 M phosphate buffer and pH = 7.4.

The temperature dependence of  $k_{\text{on}}^{\text{(fast)}}$  and  $k_{\text{on}}^{\text{(slow)}}$  were used to construct linear Eyring plots (a typical example for  $k_{\text{on}}^{\text{(fast)}}$  is shown in Figure 3), from which the activation parameters  $\Delta H^{\ddagger}_{\text{on}}$ ,  $\Delta S^{\ddagger}_{\text{on}}$ , and  $\Delta G^{\ddagger}_{\text{on}}$  for both reaction steps were calculated. As can be seen from Table 1, the values of the activation enthalpy and entropy for the fast reaction are very similar to those determined for the slow reaction; both of them appear to be

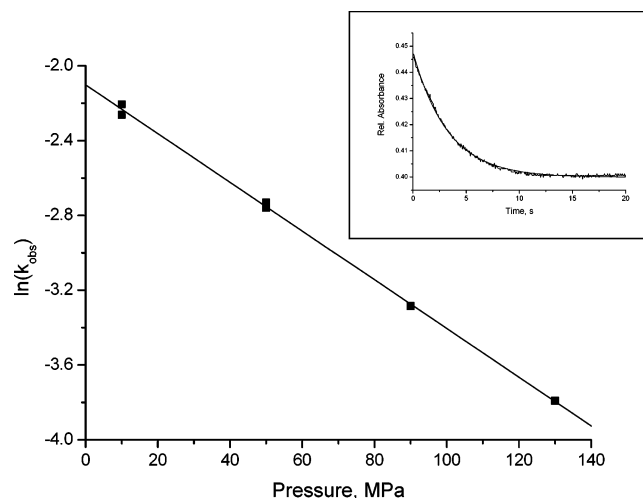
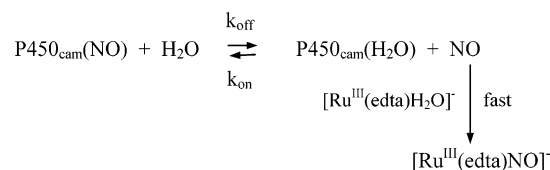


**Figure 4.** Plot of  $\ln k_{\text{obs}}$  vs pressure for the trapping of NO by  $\text{Ru}^{\text{III}}(\text{edta})\text{H}_2\text{O}^-$  from P450<sub>cam</sub>(NO) in the absence of the substrate according to the reaction outlined in Scheme 1. Experimental conditions:  $[\text{P450}_{\text{cam}}(\text{NO})] = 2.4 \times 10^{-6}$  M,  $[\text{Ru}^{\text{III}}(\text{edta})\text{H}_2\text{O}^-] = 5 \times 10^{-4}$  M in 0.1 M potassium phosphate, pH = 7.4, 20% glycerol,  $T = 25$  °C,  $\lambda_{\text{det}} = 431$  nm. Inset: Typical absorbance–time plot for the release of NO from P450<sub>cam</sub>(NO) in the absence of substrate recorded at 431 nm and 25 °C with the stopped-flow technique.

very large and positive. Significantly positive values of  $\Delta S^{\ddagger}_{\text{on}}$  are accompanied by large positive values of  $\Delta V^{\ddagger}_{\text{on}}$  from the pressure dependence of  $k_{\text{on}}$  for the fast and slow reaction steps (Table 1, Figure 3, inset).

**Kinetics of the Dissociation of NO from P450<sub>cam</sub>(NO).** The rate of NO release from the nitrosyl complex of cytochrome P450<sub>cam</sub> was measured directly by using an excess of  $[\text{Ru}^{\text{III}}(\text{edta})\text{H}_2\text{O}]^-$  to scavenge NO produced during the dissociation of P450<sub>cam</sub>(NO) according to Scheme 1.

#### Scheme 1

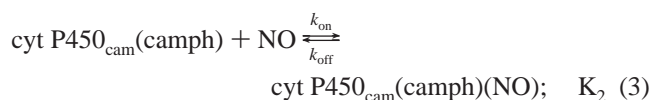


The reaction between  $[\text{Ru}^{\text{III}}(\text{edta})\text{H}_2\text{O}]^-$  and NO is very fast ( $k = 1 \times 10^8$  M<sup>-1</sup> s<sup>-1</sup> in phosphate buffer at 25 °C),<sup>27b</sup> such that under the selected experimental conditions, the release of NO from P450<sub>cam</sub>(NO) is the rate-limiting step in the reaction sequence shown in the Scheme 1, and  $k_{\text{obs}}$  can be determined directly from the observed kinetic trace, viz.,  $k_{\text{obs}} = k_{\text{off}}$ . Figure 4 (inset) shows typical Soret band spectral changes recorded at 431 nm for this reaction. The kinetic trace can be fitted to a single-exponential function, resulting in a  $k_{\text{off}}$  value of 0.35 s<sup>-1</sup> at 25 °C. The ratio  $k_{\text{on}}^{\text{(fast)}}/k_{\text{off}}$  results in the overall equilibrium constant  $K_1 = (9.26 \pm 0.03) \times 10^5$  M<sup>-1</sup>, which is in excellent agreement with the thermodynamic value of  $K_1$  determined above. The latter value does not seem to be affected by the small contribution of the slow reaction phase.

The  $k_{\text{off}}$  values determined in the temperature range 10–34.5 °C are summarized in Table 1. A linear Eyring plot of these data gave the significantly large and positive activation parameters,  $\Delta H^{\ddagger}_{\text{off}} = 122 \pm 4$  kJ mol<sup>-1</sup> and  $\Delta S^{\ddagger}_{\text{off}} = +155 \pm 15$  J mol<sup>-1</sup> K<sup>-1</sup>. The pressure dependence of  $k_{\text{off}}$  is reported in Figure 4, from which it follows that  $\Delta V^{\ddagger}_{\text{off}} = +31 \pm 1$  cm<sup>3</sup> mol<sup>-1</sup>.

**UV–vis Observations and Kinetics of the Binding of NO to Camphor-Bound Cytochrome P450<sub>cam</sub>.** Camphor binding to P450<sub>cam</sub> results in a low-spin to high-spin transformation. The spin state of the heme reflects the functional state of the enzyme, and the camphor-bound P450<sub>cam</sub> differs substantially in its coordination number, ability to undergo reduction, and optical spectra from the substrate-free form. The UV–vis spectrum of camphor-bound P450<sub>cam</sub> measured in 0.1 M potassium phosphate buffer solution at pH = 7.4 exhibits a Soret band at 391 nm ( $\epsilon = 102 \text{ mM}^{-1} \text{ cm}^{-1}$ ) and a Q-band at 515 nm ( $\epsilon = 12.5 \text{ mM}^{-1} \text{ cm}^{-1}$ ). Both of the bands are significantly blue-shifted relative to those for the substrate-free form. Addition of NO to the camphor-bound form results in the formation of a single species that is spectrally *almost* undistinguishable from that observed for NO binding to substrate-free P450<sub>cam</sub>. The only small difference between these two spectra is the position of the Soret band maximum (Figures 1a and b), which in the presence of camphor appears to be slightly (about 1.5 nm) blue-shifted to 431 nm as compared to the spectrum of P450<sub>cam</sub>(NO) recorded under the same conditions but in the absence of camphor. A similar behavior was observed earlier for the CO binding reactions to the various substrate complexes of cyt P450<sub>cam</sub>, for which a good correlation between wavenumber of the Soret band in P450<sub>cam</sub>(CO) complexes with the high spin content and the polarity of the heme pocket was found.<sup>30</sup> It was concluded that an increase in the low-spin state population (or a decrease in the high-spin content) indicates a more polar heme environment and induces a stronger Soret band red shift. This is also in good agreement with our present findings: NO binding to the substrate-free P450<sub>cam</sub> (with a small high-spin content, water molecules in heme pocket and polar environment) results in a Soret band maximum that is slightly, but significantly, red-shifted in comparison to the Soret band of cyt P450<sub>cam</sub>(NO) recorded in the presence of camphor.

As in the case of the reaction between NO and substrate-free P450<sub>cam</sub>, the release of NO from the nitrosyl complex of camphor-bound P450<sub>cam</sub> is completely reversible (Figure 1b) and consistent with eq 3:



From spectral measurements combined with the electrochemical detection of NO, the equilibrium constant  $K_2$  was calculated to be  $(1.2 \pm 0.4) \times 10^6 \text{ M}^{-1}$  at 25 °C in 0.1 M potassium phosphate buffer, pH = 7.4 and [camphor] = 0.5 mM.

**Kinetics of the “On” Reaction in the Presence of Camphor.** The binding of NO to camphor-bound cytochrome P450<sub>cam</sub> appears to be much faster than the reaction with the substrate-free form. For this reason, the kinetics of NO binding was investigated by both stopped-flow and laser flash photolysis techniques at ambient and high pressure.

**Laser Flash Photolysis Kinetics.** Irradiation at 532 nm of the P450<sub>cam</sub>(camph)(NO) solution induces dissociation of the nitrosyl complex and rapid release of NO, followed by relaxation of the system back to the original equilibrium position according to Scheme 2.

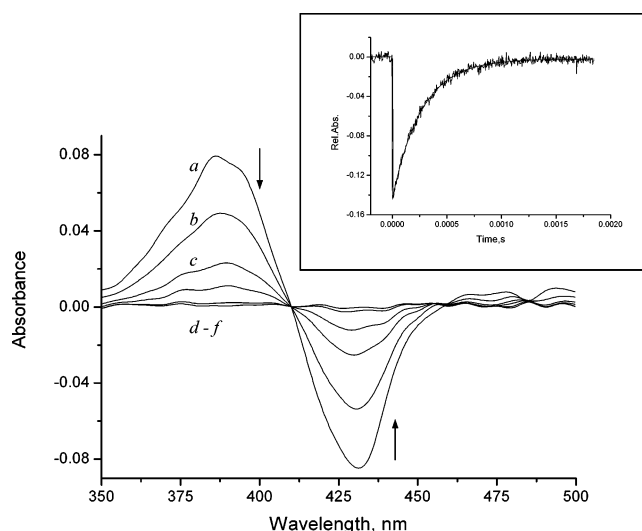
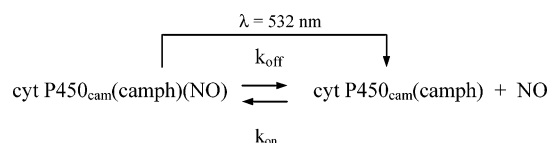


**Figure 5.** Transient absorption difference spectra for P450<sub>cam</sub>(NO) recorded following laser flash photolysis at 532 nm. Experimental conditions: [P450<sub>cam</sub>(NO)] =  $5 \times 10^{-6} \text{ M}$ , [NO] =  $0.9 \times 10^{-3} \text{ M}$  in 0.1 M potassium phosphate buffer, pH = 7.4, [camphor] =  $0.5 \times 10^{-3} \text{ M}$ ,  $T = 25 \text{ }^\circ\text{C}$ . Curves: (a) after 57  $\mu\text{s}$ ; (b) after 0.21 ms; (c) after 0.46 ms; (d) after 0.71 ms; (e) after 1.3 ms; (f) after 2.5 ms. Inset: Example of a typical flash photolysis kinetic trace recorded at 431 nm and 25 °C.

#### Scheme 2



As can be seen from Figure 5, laser flash photolysis of the equilibrium cyt P450<sub>cam</sub>(camph)(NO)/cyt P450<sub>cam</sub>(camph) mixture gave transient difference spectra consistent with the spectral differences between cyt P450<sub>cam</sub>(camph)(NO) and cyt P450<sub>cam</sub>(camph). The transient spectra decay back to the original baseline with an isosbestic point at 414 nm and with no indication of any photochemically formed side products. The decay of the transient bleaching was followed using single-wavelength detection at 431 nm and fitted to a single-exponential function (Figure 5, inset). In contrast to the reaction of NO with substrate-free P450<sub>cam</sub>, the kinetics of the binding of NO to substrate-bound P450<sub>cam</sub> clearly exhibit single-exponential behavior.

As shown in Figure 6,  $k_{\text{obs}}$  increases linearly with increasing NO concentration (eq 2) with an almost zero intercept. The slope of the plot yields  $k_{\text{on}} = (3.2 \pm 0.2) \times 10^6 \text{ M}^{-1} \text{ s}^{-1}$  at 25 °C in 0.1 M potassium phosphate buffer and pH = 7.4, which is almost 10 times larger than the binding rate constant found for substrate-free P450<sub>cam</sub> (fast phase) under the same conditions.

The temperature dependence of  $k_{\text{on}}$  (Figure 6, inset) was used to construct an Eyring plot from which the activation parameters were determined as  $\Delta H_{\text{on}}^\ddagger = 14.1 \pm 0.1 \text{ kJ mol}^{-1}$  and  $\Delta S_{\text{on}}^\ddagger = -73.1 \pm 0.4 \text{ J mol}^{-1} \text{ K}^{-1}$  (Table 2). The slope of the plot of  $\ln k_{\text{obs}}$  versus pressure (Figure 7) results in  $\Delta V_{\text{on}}^\ddagger = -7.3 \pm 0.2 \text{ cm}^3 \text{ mol}^{-1}$ . As can be seen from the data summarized in Tables 1 and 2, the values of the activation parameters found for the binding of NO to camphor-bound P450<sub>cam</sub> are negative and significantly smaller in absolute values than those obtained for the reaction with the substrate-free form of the enzyme.

**Stopped-Flow Kinetics.** Because NO binds very rapidly to camphor-bound P450<sub>cam</sub>, the temperature and pressure depen-

(30) Jung, C.; Schulze, H.; Deprez, E. *Biochemistry* **1996**, *35*, 15088.

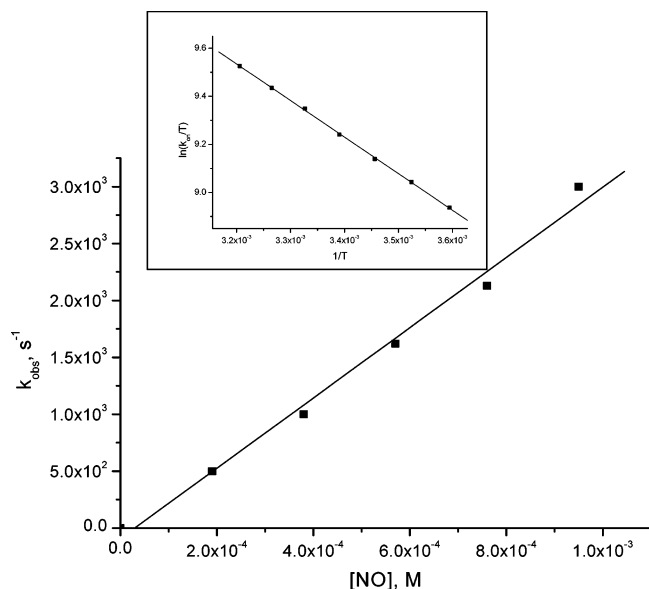


**Figure 6.** NO concentration dependence of  $k_{\text{obs}}$  (at 25 °C) and temperature dependence of  $k_{\text{on}}$  (inset) for the binding of NO to camphor-bound P450<sub>cam</sub> as measured by laser flash photolysis technique. Experimental conditions: [P450<sub>cam</sub>] =  $5 \times 10^{-6}$  M in 0.1 M potassium phosphate buffer, pH = 7.4, [camphor] =  $0.5 \times 10^{-3}$  M,  $\lambda_{\text{irr}} = 532$  nm,  $\lambda_{\text{det}} = 431$  nm.

**Table 2.** Rate Constants and Activation Parameters for NO Binding to Camphor-Bound P450<sub>cam</sub> As Determined by Stopped-Flow and Laser Flash Photolysis.

T/°C	P/MPa	"on" reaction		"off" reaction
		$k_{\text{on}}$ (stopped-flow) ( $\times 10^{-3}$ ) M <sup>-1</sup> s <sup>-1</sup>	$k_{\text{on}}$ (flash photolysis) ( $\times 10^{-3}$ ) M <sup>-1</sup> s <sup>-1</sup>	$k_{\text{off}}$ s <sup>-1</sup>
5.0	0.1		21.1 ± 0.2	0.15 ± 0.01
10.0			24.0 ± 0.1	
15.0		27.8 ± 0.5	26.8 ± 0.5	0.58 ± 0.04
20.0		30.2 ± 0.9	30.2 ± 0.3	
25.0		34.5 ± 0.9	32.3 ± 0.5	1.93 ± 0.02
30.0		38 ± 2	37.9 ± 0.2	
35.0			42.2 ± 0.7	5.68 ± 0.07
40.0			12.4 ± 0.2	
5.0	10	22.8 ± 0.1		
	50	25.5 ± 0.1		
	90	28.0 ± 0.1		
	130	32.4 ± 0.2		
25.0	10		32.2 ± 0.3	1.50 ± 0.03
	40		35.3 ± 0.3	
	50			0.99 ± 0.05
	70		38.6 ± 0.3	
	90			0.68 ± 0.04
	100		42.8 ± 0.3	
	130		45.4 ± 0.7	0.50 ± 0.05
$\Delta H^\ddagger$ kJ mol <sup>-1</sup>		13.6 ± 1.1	14.1 ± 0.1	83.8 ± 0.7
$\Delta S^\ddagger$ J mol <sup>-1</sup> K <sup>-1</sup>		-74 ± 4	-73.1 ± 0.4	+41 ± 2
$\Delta V^\ddagger$ cm <sup>3</sup> mol <sup>-1</sup>		-6.5 ± 0.4	-7.3 ± 0.2	+24 ± 1

dence of the "on" reaction could also be studied using stopped-flow techniques but only at low NO concentrations. The values of  $k_{\text{on}}$  determined for the temperature range 15 to 30 °C and pressure range 10–130 MPa are listed in Table 2. The respective activation parameters obtained from these data are in reasonable agreement with those reported above for the laser flash photolysis experiments.

**Kinetics of the Dissociation of NO from P450<sub>cam</sub>(camphor)(NO).** The dissociation rate constants,  $k_{\text{off}}$ , were determined by stopped-flow mixing of a P450<sub>cam</sub>(camphor)(NO) buffered solution with an excess of [Ru<sup>III</sup>(edta)H<sub>2</sub>O]<sup>-</sup> as NO-scavenger (see Scheme 1). Spectral changes were monitored at 431 nm (Figure

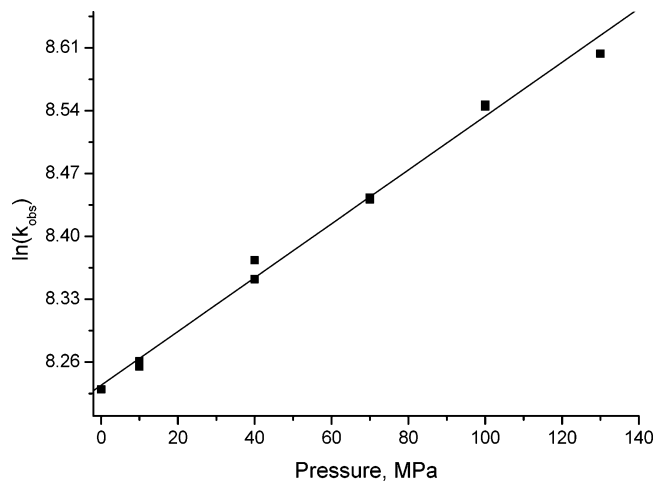


**Figure 7.**  $k_{\text{obs}}$  as a function of pressure for the reaction between camphor-bound P450<sub>cam</sub> and NO as measured by laser flash photolysis. Experimental conditions: [P450<sub>cam</sub>] =  $5.6 \times 10^{-6}$  M, [NO] =  $9.5 \times 10^{-4}$  M in 0.1 M potassium phosphate buffer, pH = 7.4, [camphor] =  $0.5 \times 10^{-3}$  M,  $T = 25$  °C,  $\lambda_{\text{irr}} = 532$  nm,  $\lambda_{\text{det}} = 431$  nm.

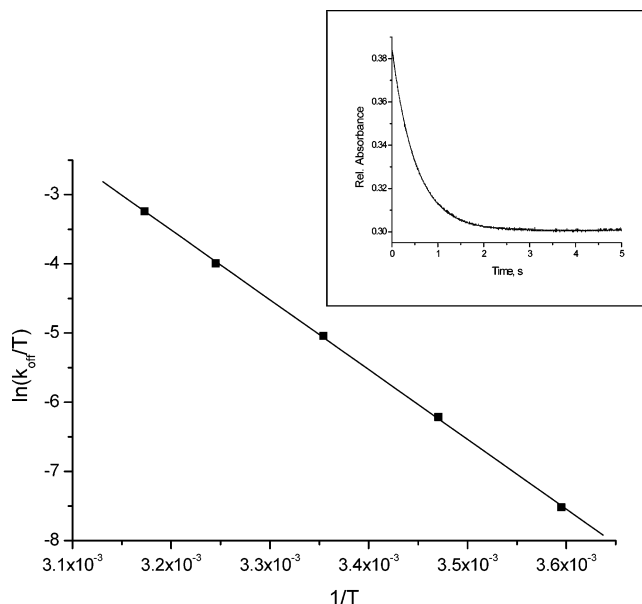


**Figure 8.** NO release from P450<sub>cam</sub>(NO) in the presence of camphor recorded on the stopped-flow instrument as a function of temperature. Experimental conditions: [P450<sub>cam</sub>(NO)] =  $1.2 \times 10^{-6}$  M, [Ru<sup>III</sup>(edta)H<sub>2</sub>O]<sup>-</sup> =  $5 \times 10^{-4}$  M, [camphor] =  $0.5 \times 10^{-3}$  M in 0.1 M potassium phosphate buffer, pH = 7.4,  $\lambda_{\text{det}} = 431$  nm. Inset: Absorbance–time plot for NO dissociation from P450<sub>cam</sub>(NO) recorded at 431 nm and 25 °C ( $k_{\text{obs}} = 1.93$  s<sup>-1</sup>).

8, inset), and the  $k_{\text{off}}$  values determined in the temperature range from 5 to 35 °C are summarized in Table 2. A linear Eyring plot of the data (Figure 8) resulted in the values  $\Delta H^\ddagger_{\text{off}} = 83.1 \pm 0.7$  kJ mol<sup>-1</sup> and  $\Delta S^\ddagger_{\text{off}} = +41 \pm 2$  J mol<sup>-1</sup> K<sup>-1</sup>. A plot of  $\ln k_{\text{off}}$  versus pressure is linear, from which it follows that  $\Delta V^\ddagger_{\text{off}} = +24 \pm 1$  cm<sup>3</sup> mol<sup>-1</sup>.

## Discussion

**Equilibrium and Rate Constants for NO Binding to Substrate-Free P450<sub>cam</sub>.** The binding of NO to substrate-free P450<sub>cam</sub> displays biphasic kinetics in which the major contribution (~90%) comes from the fast reaction step. This biphasic behavior can be interpreted in terms of an equilibrium between conformational substates in cytochrome P450<sub>cam</sub>. Multiple

**Table 3.** Rate Constants  $k_{\text{on}}$  and  $k_{\text{off}}$  for NO Binding to Ferriheme Proteins

ferric proteins <sup>a</sup>	$k_{\text{on}}$ M <sup>-1</sup> s <sup>-1</sup>	$k_{\text{off}}$ s <sup>-1</sup>	conditions	ref
eNOS <sup>b</sup>	$6.1 \times 10^5$	93	at 10 °C, pH = 7.4, stopped-flow kinetics, $k_{\text{off}}$ values determined from the intercept of the plot of $k_{\text{obs}}$ vs [NO]	20c
eNOS <sup>c</sup>	$8.2 \times 10^5$	70		
nNOS <sup>d</sup>	$1.9 \times 10^7$	50	at 23 °C, Tris buffer, pH 7.8, laser flash photolysis; $k_{\text{off}}$ determined from the intercept of the plot of $k_{\text{obs}}$ vs [NO]	20a
		5	$k_{\text{off}}$ determined by NO-trapping method using MbO <sub>2</sub> as NO scavenger	
nNOS <sup>e</sup>	$6.1 \times 10^6$	60	at 23 °C, Tris buffer, pH 7.8, laser flash photolysis; $k_{\text{off}}$ determined from the intercept of the plot of $k_{\text{obs}}$ vs [NO]	
		2	$k_{\text{off}}$ determined by NO-trapping method using MbO <sub>2</sub> as NO scavenger	
P 450 <sub>nor</sub>	$1.9 \times 10^7$		at 20 °C, sodium phosphate buffer, pH = 7.2, laser flash photolysis	19
P 450 <sub>1A2</sub>	$1.7 \times 10^4$	0.15	at 25 °C, potassium phosphate, pH = 7.4, laser flash photolysis	18
	$1.9 \times 10^5$	0.51	in the presence of the substrate (7-ethoxycoumarin)	
metMb	$4.8 \times 10^4$	28.9	at 25 °C, Tris buffer, pH = 7.4, stopped-flow	21

<sup>a</sup> Abbreviations: eNOS, endothelial nitric oxide synthase; nNOS, neuronal nitric oxide synthase; P450<sub>nor</sub>, nitric oxide reductase; H4B, (6R)-5,6,7,8-tetrahydro-L-biopterin; P 450<sub>1A2</sub>, cytochrome P450 from yeast (*Saccharomyces cerevisiae*); metMb, metmyoglobin from equine heart. <sup>b</sup> H4B-saturated eNOS in the absence of the substrate. <sup>c</sup> H4B-saturated eNOS in the presence of arginine. <sup>d</sup> Heme domain in the presence of H4B. <sup>e</sup> Holoenzyme in the presence of H4B.

conformations in P450 have already been confirmed and extensively studied by FTIR.<sup>17f,30–33</sup> These studies indicate that the different substates in substrate-free P450<sub>cam</sub> are caused by a different hydrogen bonding network between differently packed water molecules in the heme pocket.<sup>30,31</sup> On the binding of NO to the heme iron, the coordinated water molecule must dissociate, which will be accompanied by the rearrangement of the other water molecules in the heme pocket. These processes may occur at different rates for the different substates and seem to be the rate-limiting steps for the binding of NO. Water dissociation is characterized by very positive activation entropies (see Table 1) typical for such processes, and the difference in  $\Delta S^\ddagger$  for the two reaction steps can account for the difference of a factor of ca. 60 (at 25 °C) between the values of  $k_{\text{on}}$  for the two reaction steps. The activation entropies suggest a loosening of the water cluster in the heme pocket on dissociation of the coordinated water molecule.

As can be seen from the data reported in Table 3, NO binds much faster to nitric oxide synthase (endothelial or neuronal) and nitric oxide reductase than to substrate-free P450<sub>cam</sub>. In contrast, the reactivity of NO toward substrate-free cytochrome P450<sub>1A2</sub> from *Saccharomyces cerevisiae* was found to be much lower than that of cyt P450<sub>cam</sub>. Since in all these systems NO binds to the thiolate-ligated iron(III) center, the apparent difference in the NO substitution kinetics could be explained in terms of the different protein architecture of their heme active sites and/or the lability/absence of a ligand that can leave the iron center. These properties seem to correlate very well with the biological functions and difference in the catalytic activity of these enzymes.<sup>19,20</sup> Comparison of the NO association rate constant obtained for the iron(III) thiolate-ligated heme proteins with those found for systems that possess an imidazole proximal ligand (e.g., NO binding to metmyoglobin<sup>21</sup>) led to the conclusion that thiolate ligation to the Fe(III) heme center has only a minor influence on the nitrosylation rate constants. It was shown by Magde et al.<sup>20a</sup> that proximal cysteine ligation in nitric oxide synthase makes the NO binding kinetics to ferric and ferrous species more similar (i.e., the rate constants for NO association were found to be very fast and similar for both ferric and ferrous NOS derivatives) than that observed for the imidazole-ligated

systems. In general it is true that the anionic nature of the RS<sup>-</sup> group in the proximal position of the thiolate-ligated heme proteins should stabilize the iron atom in its higher (Fe<sup>III</sup>) oxidation state and therefore affect the ligation kinetics of these systems. However, as can be seen from Table 3, Fe(III) heme proteins with even the same thiolate ligation can exhibit quite a wide range of NO binding rate constants. It seems that other factors mentioned above, like the lability of the leaving group (or its absence) or the protein structure and accessibility of the heme active site, play a crucial role in the dynamics of the reactions of NO with metal centers of biological relevance.

In contrast to the NO binding reaction, which exhibits two distinct phases separated in rate by a factor of about 55 at 25 °C, the NO dissociation reaction displays only single-exponential kinetics. This behavior can be explained by assuming that the breakage of the Fe–NO bond is the rate-limiting process. This suggests that the possible rearrangement of the water cluster in the heme pocket does not play a significant role during the dissociation of NO. The NO dissociation rate constant determined in the present study for the nitrosyl complex of substrate-free P450<sub>cam</sub> is very similar to that found for P450<sub>1A2</sub>(NO)<sup>18</sup> and much smaller than those obtained for the nitrosyl complexes of nitric oxide synthase<sup>20a,c</sup> and metmyoglobin<sup>21</sup> (Table 3). Hence, the real difference between the *trans* effects of proximal imidazole and thiolate coordination in such systems seems to be more complex. It is suggested that ligand dissociation rate constants are largely affected by the nature of the binding of NO and the dissociation mechanism, as well as by factors that can stabilize NO binding in the protein active site (e.g., stabilization of NO by distal histidine observed in many nitrosyl complexes of myoglobin or hemoglobin).

The nitrosyl complex of substrate-free P450<sub>cam</sub> appears to be much more stable than the nitrosyl complexes of metmyoglobin and cytochrome P450<sub>1A2</sub> due to its relatively high  $k_{\text{on}}^{(\text{fast})}$  value and low dissociation rate constant. In the case of the ferric neuronal and endothelial NO synthases, the affinity for NO is almost comparable to that of cytochrome P450<sub>cam</sub>. Although the association rates for ferric nNOS and eNOS are quite fast, of the order of  $1 \times 10^7 \text{ M}^{-1} \text{ s}^{-1}$  at 25 °C,<sup>20a</sup> the stability constants  $K_{\text{NO}}$  seem to be rather modest, due exclusively to rapid NO dissociation from the nitrosyl complexes of these proteins (Table 3). Since nitric oxide synthase is involved in the NO regulatory cycle, the reasonably low affinity for NO is closely

(31) Jung, C.; Ristau, O.; Schulze, H.; Sliagar, S. G. *Eur. J. Biochem.* **1996**, *235*, 660.

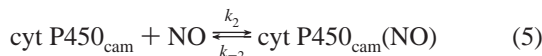
(32) Schulze, H.; Ristau, O.; Jung, C. *Eur. J. Biochem.* **1994**, *224*, 1047.

(33) Jung, C. *J. Mol. Recognit.* **2000**, *13*, 325.



connected with the biological functions of this enzyme: rapid NO dissociation rates keep NOS from being poisoned, whereas fast association rates allow rapid reactions with NO in the case of the overproduction of NO.<sup>20a</sup>

**Mechanistic Interpretation of NO Binding to Substrate-Free P450<sub>cam</sub>.** NO binding to both subconformers of substrate-free P450<sub>cam</sub> is characterized by rather similar activation parameters (see Table 1). The values of the activation entropy and volume for both reaction steps were found to be large and positive, typical for a dissociative ligand substitution mechanism according to reactions 4 and 5:



If the steady-state approximation is applied to the five-coordinate high-spin intermediate cyt P450<sub>cam</sub>, the expression for the observed first-order rate constant is given in eq 6:

$$k_{\text{obs}} = \frac{k_1 k_2 [\text{NO}] + k_{-1} k_{-2} [\text{H}_2\text{O}]}{k_{-1} [\text{H}_2\text{O}] + k_2 [\text{NO}]} \quad (6)$$

Since  $[\text{H}_2\text{O}] \gg [\text{NO}]$  and both  $k_{-1}$  and  $k_2$  involve the trapping of the intermediate cyt P450<sub>cam</sub>, it may be concluded that  $k_{-1}[\text{H}_2\text{O}] \gg k_2[\text{NO}]$  in the absence of any significant curvature in the  $[\text{NO}]$ -dependence of  $k_{\text{obs}}$ . Therefore, eq 6 can be simplified to

$$k_{\text{obs}} = \frac{k_1 k_2 [\text{NO}]}{k_{-1} [\text{H}_2\text{O}]} + k_{-2} \quad (7)$$

where  $k_{\text{on}} = k_1 k_2 / k_{-1} [\text{H}_2\text{O}]$  and  $k_{\text{off}} = k_{-2}$ . Under such conditions the dissociation of water can also be treated as a rapid preequilibrium, i.e.,  $k_{\text{on}} = K_1 k_2 / [\text{H}_2\text{O}]$ , where the equilibrium lies far to the left side of reaction 4 because  $k_{-1}[\text{H}_2\text{O}] \gg k_2[\text{NO}]$ . This means that NO competes with the rapid water exchange process on cyt P450<sub>cam</sub>(H<sub>2</sub>O) to bind to the Fe(III) center. Taking into account that  $k_{-1}$  and  $k_2$  represent the binding of small, neutral molecules (H<sub>2</sub>O or NO) to the five-coordinate metal center, the difference in their activation parameters (i.e.,  $\Delta H^\ddagger_2 - \Delta H^\ddagger_{-1}$ ,  $\Delta S^\ddagger_2 - \Delta S^\ddagger_{-1}$ , and  $\Delta V^\ddagger_2 - \Delta V^\ddagger_{-1}$ ) are expected to be small. Thus, the activation parameters for  $k_{\text{on}}$  are largely determined by the dissociation of the water molecule from cyt P450<sub>cam</sub>(H<sub>2</sub>O) ( $k_1$  pathway) to form the five-coordinate, high-spin intermediate. Dissociation of a coordinated water molecule from an octahedral metal center is expected to be accompanied by a maximum volume increase of 13 cm<sup>3</sup> mol<sup>-1</sup>.<sup>34</sup> However, this reaction also involves a change in spin state from the six-coordinate, low-spin aqua complex ( $S = 1/2$ , doublet) to the five-coordinate, high-spin P450<sub>cam</sub> intermediate ( $S = 5/2$ , sextet). In this context, the activation volume for  $k_{\text{on}}$  should not only include a volume increase due to Fe<sup>III</sup>–H<sub>2</sub>O bond breakage but also a volume increase associated with the low-spin  $\rightarrow$  high-spin transition. It was previously shown<sup>35</sup> for metMb-L systems

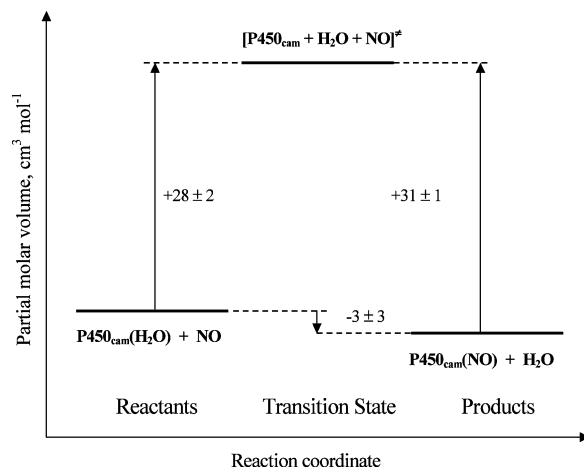


**Figure 9.** Volume profile for the reversible binding of NO to substrate-free cytochrome P450<sub>cam</sub>.

that the low-spin  $\rightarrow$  high-spin transformation is accompanied by a volume increase of 12–15 cm<sup>3</sup> mol<sup>-1</sup>. As a result, the overall volume of activation for the “on” reaction can be expected to be as large as +25 to +28 cm<sup>3</sup> mol<sup>-1</sup>, which is very close to the experimental value, viz.,  $\Delta V^\ddagger_{\text{on}} = +28 \pm 2$  cm<sup>3</sup> mol<sup>-1</sup>. The large value of  $\Delta V^\ddagger_{\text{on}}$  also corresponds well with the large and positive value of  $\Delta S^\ddagger_{\text{on}}$  ( $+169 \pm 4$  J mol<sup>-1</sup> K<sup>-1</sup>), consistent with the limiting dissociative mechanism outlined in reactions 4 and 5.

Notably, the  $k_2$  pathway (reaction 5) also involves a change in spin state. The nitrosyl complex of P450<sub>cam</sub> (in the presence or absence of substrate) is a diamagnetic species.<sup>4</sup> This means that binding of NO to the high-spin, five-coordinate intermediate must also involve a change in the spin state from a sextet ( $S = 5/2$ ) to a diamagnetic complex,  $S = 0$ . Resonance Raman studies<sup>14</sup> revealed that the Fe–NO linkage in the nitrosyl complex of the substrate-free form of cyt P450<sub>cam</sub> adopts a linear structure. This indicates that during the bond-formation process ( $k_2$  pathway), partial charge transfer from NO to Fe<sup>III</sup> occurs to give a linearly bound diamagnetic {FeNO}<sup>6</sup> complex, which can be formally presented as Fe<sup>II</sup>–NO<sup>+</sup>.

The activation parameters for the release of NO were also found to be large positive values (Table 1). These values clearly show that the “off” reaction also follows a rate-limiting dissociative mechanism (reactions 4 and 5) in agreement with the principle of microscopic reversibility. For the reverse reaction, the  $k_{-2}$  pathway seems to be the energetically dominant step. It involves breakage of the iron–nitrosyl bond, accompanied by a formal oxidation of Fe<sup>II</sup> to Fe<sup>III</sup> and solvent reorganization due to charge redistribution around the Fe<sup>II</sup>–NO<sup>+</sup> species. Moreover, the loss of NO from the nitrosyl complex and formation of the unsaturated five-coordinate intermediate (pathway  $k_{-2}$ ) is associated with a change in the spin state on iron from low-spin to high-spin. All these factors are consistent with the large and positive values of the activation entropy and activation volume found in the present study.

As can be seen from Figure 9, the overall reaction volume for the binding of NO to substrate-free cytochrome P450<sub>cam</sub> is very small and can be interpreted as close to zero ( $\Delta V = -3 \pm 3$  cm<sup>3</sup> mol<sup>-1</sup>). A similar scenario was observed earlier for the reaction between NO and the imidazole-ligated ferric hemo-protein, metmyoglobin.<sup>21</sup> The overall volume change determined for this system was also close to zero ( $\Delta V = 5 \pm 2$  cm<sup>3</sup> mol<sup>-1</sup>),

(34) (a) Drljaca, A.; Hubbard, C. D.; van Eldik, R.; Asano, T.; Basilevsky, M. V.; le Noble, W. J. *Chem. Rev.* **1998**, *98*, 2167. (b) Stochel, G.; van Eldik, R. *Coord. Chem. Rev.* **1999**, *187*, 329.

(35) (a) Messana, C.; Cerdonio, M.; Shenkin, P.; Noble, R.; Fermi, G.; Perutz, R. N.; Perutz, M. F. *Biochemistry*, **1978**, *17*, 3652. (b) Morishima, I.; Ogawa, S.; Yamada, H. *Biochemistry* **1980**, *19*, 1569.

although the reported value for  $\Delta V_{\text{on}}^{\ddagger}$ , representing volume changes associated with the  $k_1$  pathway, was found to be a bit smaller (viz.,  $21 \text{ cm}^3 \text{ mol}^{-1}$ ) than that obtained for the present system. On the other hand, the values of the activation volume for the “on” reaction reported for model porphyrin systems<sup>36</sup> are significantly smaller in comparison to those found for the substrate-free cyt P450<sub>cam</sub>/NO and metmyoglobin/NO systems. It is suggested that the larger values of  $\Delta V_{\text{on}}^{\ddagger}$  reported for NO binding to hemoproteins in comparison to the reactions with porphyrin model systems may be due to the fact that the protein can also undergo some structural rearrangement during the formation of the five-coordinate intermediate ( $k_1$  pathway) and involve a change in spin state.

**Effect of Camphor on the Binding of NO to Cytochrome P450<sub>cam</sub>.** In the presence of camphor, NO binding to P450<sub>cam</sub> exhibits single-exponential kinetics. As shown by Jung et al., many of the substrate-bound complexes (e.g., 1R-camphor, norcamphor, norbornane) appear as a single substrate at room temperature.<sup>30</sup> This can be explained in terms of the transitions between different substates of cytochrome P450<sub>cam</sub>, which at room temperature become very fast and shift the equilibrium to only one subconformer. A different behavior was observed for the substrate-free cytochrome P450<sub>cam</sub>, whose conformational substates even at room temperature can be classified in two main subconformer ensembles.<sup>30, 31</sup>

As can be seen from the data summarized in Tables 1 and 2, camphor binding to cytochrome P450<sub>cam</sub> markedly accelerates (about a factor of 10) NO association to the heme iron(III) center of this protein. Similar behavior was also observed for the binding of NO to the ferric wild-type P450<sub>1A2</sub> enzyme, for which the presence of substrates (7-ethoxycoumarin, anthracene, phenanthrene, and dibenzanthracene) also increased the NO association rate constants ( $k_{\text{on}}$ ) by a factor from 2- to 11-fold.<sup>18</sup> In contrast, it was shown<sup>17a</sup> for the P450<sub>cam</sub>/CO systems that substrate binding to P450<sub>cam</sub> (e.g., complexes with 1R-camphor, norcamphor, camphane, or norbornane) significantly decreased the association rate constants of CO to ferrous P450<sub>cam</sub> by a factor up to 10-fold. It seems that the apparent differences in the substrate effects observed in the binding kinetics of NO and CO can easily be explained in terms of the difference in the coordination sphere of cytochrome P450<sub>cam</sub> in the oxidized and reduced states and in the presence and absence of substrate (see further discussion).

The presence of camphor markedly affects not only the NO association rate constants but also NO release from the nitrosyl complex of P450<sub>cam</sub> (Table 2). The value of the dissociation rate constant determined in the NO-trapping experiments is ca. 5 times larger than the value of  $k_{\text{off}}$  found under the same conditions but in the absence of camphor. The ratio of  $k_{\text{on}}/k_{\text{off}}$  for the reaction of NO with camphor-bound P450<sub>cam</sub> (eq 3) results in  $K_2 = (1.7 \pm 0.2) \times 10^6 \text{ M}^{-1}$  at 25 °C and shows a good agreement within the experimental error limits with the thermodynamic value,  $(1.2 \pm 0.4) \times 10^6 \text{ M}^{-1}$ , found under the same conditions. ON the basis of the fact that NO binds 10 times faster to camphor-bound P450<sub>cam</sub> and also dissociates from this complex ca. 5 times faster than in the case of the substrate-free form, the nitrosyl adduct of P450<sub>cam</sub> in the presence of

camphor appears to be ca. two times more stable than the P450<sub>cam</sub>(NO) complex in the absence of camphor.

**Mechanism of NO Binding to Cytochrome P450<sub>cam</sub> in the Presence of Camphor.** The binding of the natural substrate 1R-camphor to low-spin, six-coordinate P450<sub>cam</sub> causes a change in spin state to approximately 100% of the high-spin form. The resulting complex is five-coordinate with no water molecule occupying the sixth position of the heme-iron(III) center. Since the Fe<sup>III</sup>-heme center is five-coordinate, formation of an Fe–NO bond does not require initial displacement of a water molecule and therefore the ligation reaction cannot be limited by the rate of water dissociation as was observed for the reaction with substrate-free P450<sub>cam</sub>. On this basis, second-order rate constants for the binding of NO to camphor-bound P450<sub>cam</sub> can be much larger than those determined for substrate-free P450<sub>cam</sub>. A different scenario is observed when CO binds to ferrous cytochrome P450<sub>cam</sub>. Since the Fe<sup>II</sup>-heme center is five-coordinate in P450<sub>cam</sub>, a water molecule no longer occupies the proximal position, regardless of the presence or the absence of camphor in the heme pocket. This means that in this case the coordination sphere of the heme-iron center cannot account for the different CO association rate constants observed for the reactions with substrate-free and substrate-bound P450<sub>cam</sub>. As suggested by Jung et al.,<sup>17a</sup> the values of the second-order rate constants reported for the binding of CO correlate very well with the compressibility and the influx rate of water molecules into the heme pocket of P450<sub>cam</sub>. In the case of CO association with substrate-free P450<sub>cam</sub> (or loosely bound substrate complexes), the high solvent accessibility of the heme pocket and a very compressible active site make the reaction entropically favored and therefore very fast ( $k_{\text{on}} \approx 3 \times 10^6 \text{ M}^{-1} \text{ s}^{-1}$  at 5 °C).<sup>17a</sup> In contrast, binding of camphor (or other substrates of class I possessing methyl groups) to cytochrome P450<sub>cam</sub> causes the protein and the heme pocket to be more rigid and less compressible. As a result, CO binding to camphor-bound P450<sub>cam</sub> is disfavored and is 2 orders of magnitude slower ( $k_{\text{on}} \approx 3 \times 10^4 \text{ M}^{-1} \text{ s}^{-1}$  at 5.6 °C)<sup>17a</sup> than that observed for the reaction with the substrate-free form.

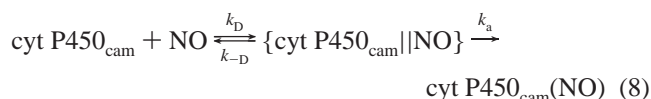
In the case of NO binding to ferric P450<sub>cam</sub>, the reaction was found to be much faster in the presence of camphor than in its absence. This can be easily ascribed, as already mentioned, to the vacant position in the coordination sphere of the substrate-bound Fe<sup>III</sup>-heme. However, but it is not clear what effects on the  $k_{\text{on}}$  values could be expected from the protein and heme pocket, which become more rigid and inflexible following binding of camphor. It is likely that in the present case these two opposite effects (i.e., facilitation of NO binding due to a vacant coordination site and slowing down the binding rate due to rigidity of the active site) play important roles. Taking into account that the “on” rates for the reaction of NO with *five-coordinate* ferrous hemoproteins are about 3 orders of magnitude larger than those for the *six-coordinate* ferric analogues (e.g., NO binds to deoxymyoglobin and metmyoglobin with rate constants of  $1.7 \times 10^7 \text{ M}^{-1} \text{ s}^{-1}$ <sup>37</sup> and  $4.8 \times 10^4 \text{ M}^{-1} \text{ s}^{-1}$ ,<sup>21</sup> respectively), the effect of the vacant sixth coordination position in camphor bound P450<sub>cam</sub> does not seem to be so large, since the NO binding rate constant is only 10 times larger in the presence of camphor than in its absence. The partial compensa-

(36) Lavermann, L. E.; Hoshino, M.; Ford, P. C. *J. Am. Chem. Soc.* **1997**, *119*, 12663.

(37) DiBenedetto, J. D.; Arkle, V.; Goodwin, H. A.; Ford, P. C. *Inorg. Chem.* **1985**, *24*, 455.

tion of the two opposite effects could account for such a behavior. Another possible reason for the small difference between the NO binding rate constants for five- and six-coordinate iron(III) in cyt P450<sub>cam</sub> can be the difference in the reorganization of the spin multiplicity observed for these complexes during the reaction with NO. The spin states of the substrate-free and camphor-bound P450<sub>cam</sub> are  $S = 1/2$  and  $5/2$ , respectively, whereas that of the nitrosyl P450<sub>cam</sub> complex is  $S = 0$  in both cases. This means that NO binding to camphor-bound P450<sub>cam</sub> results in a larger reorganization of spin multiplicity than for the substrate-free analogue. In this respect it was shown by Hoshino et al.<sup>40</sup> for a series of model porphyrin complexes, M(TPP) where M = Mn<sup>II</sup>, Fe<sup>II</sup>, and Co<sup>II</sup>, TPP = *meso*-tetraphenylporphyrin, that the smallest NO binding rate constant is found for complexes that have to undergo the largest reorganization of the spin multiplicity.

The activation parameters for the formation of the nitrosyl complex of P450<sub>cam</sub> in the presence of camphor show a good agreement between measurements made by using stopped-flow and laser flash photolysis techniques (Table 2). The  $\Delta H_{\text{on}}^{\ddagger}$  values were found to be much lower than in the reaction with the substrate-free form, and the values of the activation entropy and activation volume are much more negative, viz.,  $\Delta S_{\text{on}}^{\ddagger} = -74 \pm 4 \text{ J mol}^{-1} \text{ K}^{-1}$  and  $\Delta V_{\text{on}}^{\ddagger} = -6.9 \pm 0.6 \text{ cm}^3 \text{ mol}^{-1}$  (mean values from stopped-flow and laser flash photolysis measurements). These features are consistent with the mechanism proposed earlier for the reaction of NO with ferro-heme proteins<sup>38</sup> and model compounds.<sup>39</sup> In such a mechanism an encounter complex, {Fe(Por)||L}, is formed prior to ligand bond formation, i.e.



where  $k_D$  is the rate constant for the diffusion-limited formation of the encounter complex,  $k_{-D}$  is the rate constant for diffusion apart of the encounter complex, and  $k_a$  is that for the “activation” step in which the Fe–NO bond is formed. There are two limiting cases for reaction 8: one consistent with a diffusion-controlled process ( $k_a \gg k_{-D}$ ) and the other one typical for an activation-controlled process ( $k_{-D} \gg k_a$ ). The value of the second-order rate constant,  $k_{\text{on}}$ , for the binding of NO to camphor-bound cyt P450<sub>cam</sub> was found to be  $(3.23 \pm 0.05) \times 10^6 \text{ M}^{-1} \text{ s}^{-1}$  at 25 °C, which is many orders of magnitude smaller than for diffusion-controlled reactions in water. The negative values found for the activation entropy and, more significantly, the activation volume are consistent with an activation-controlled reaction mechanism, i.e., rate-determining Fe<sup>III</sup>–NO bond formation. In such a case, Fe<sup>III</sup>–NO bond formation and the concomitant change in spin state from high (sextet cyt P450<sub>cam</sub>,  $S = 5/2$  plus doublet NO,  $S = 1/2$ ) to low spin (singlet cyt P450<sub>cam</sub>(NO),  $S = 0$ ) should result in negative contributions to the activation entropy and activation volume. By comparison, these parameters were found to be large and positive for the

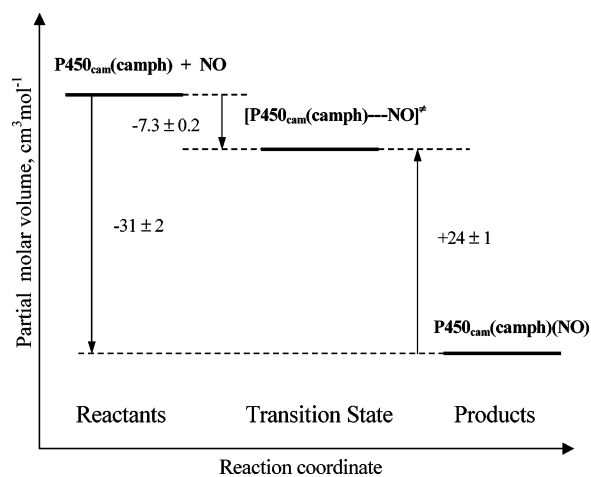


**Figure 10.** Volume profile for the reversible binding of NO to camphor-bound cytochrome P450<sub>cam</sub>.

release of NO from the nitrosyl complex of camphor-bound P450<sub>cam</sub>. As can be seen from Table 2, the value of the activation volume is especially large, viz.,  $\Delta V_{\text{off}}^{\ddagger} = +24 \pm 1 \text{ cm}^3 \text{ mol}^{-1}$ . These activation parameters are consistent with a reaction mechanism in which the iron-nitrosyl bond is broken. Since in the P450<sub>cam</sub>(NO) complex, Fe<sup>III</sup>–NO has Fe<sup>II</sup>–NO<sup>+</sup> character, Fe–NO bond cleavage should formally be accompanied by charge transfer from the metal to the nitrosyl ligand, i.e., a formal oxidation of Fe<sup>II</sup> to Fe<sup>III</sup> and solvational changes as a result of charge redistribution. During this process the spin state of iron changes from low spin ( $S = 0$ ) to high spin ( $S = 5/2$ ), which will result in a considerable positive contribution to the value of  $\Delta V_{\text{off}}^{\ddagger}$ .

The negative activation volume found for the “on” reaction and the large and positive value found for the reverse “off” reaction result in a large and negative reaction volume,  $\Delta V = -31 \pm 2 \text{ cm}^3 \text{ mol}^{-1}$ . As can be seen from Figure 10, the volume profile for the reaction between NO and camphor-bound P450<sub>cam</sub> differs totally from that obtained for the binding of NO to the substrate-free form (Figure 9). In this case the volume profile indicates a drastic volume decrease on going from the reactant to the product states, which can be partly ascribed to the high spin to low spin transition of the Fe(III) during the binding of NO. It should also be noted that the transition state for the “on” reaction can be described as “early”, i.e., close in nature to the reactant state, which indicates that partial bond formation with NO accounts for this position. Subsequently, bond formation is completed and accompanied by the formal high-spin to low-spin change. Thus the volume profiles in Figures 9 and 10 differ significantly and nicely demonstrate the importance of bond-formation/bond-breakage processes coupled to changes in the spin state of the Fe(III) center for the interaction with NO.

**Acknowledgment.** Studies at the University of Erlangen-Nürnberg were supported by the Deutsche Forschungsgemeinschaft (SPP 1118). Studies at the Jagiellonian University were supported by the Foundation for Polish Science (“Fastkin” no. 8/97). Studies at the Max-Delbrück Center for Molecular Medicine were supported by the Deutsche Forschungsgemeinschaft (SK 35/3-5 and Ju 229/4-2). We thank Jörg Contzen (MDC) for performing the substrate removal from P450<sub>cam</sub>.

JA038774D

(38) (a) Taube, D. J.; Projahn, H. D.; van Eldik, R.; Magde, D.; Traylor, T. G. *J. Am. Chem. Soc.* **1990**, *112*, 6880. (b) Ansari, A.; Jones, C. M.; Henry, E. R.; Hofrichter, J.; Eaton, W. A. *Biochemistry* **1994**, *33*, 5128. (c) Tétreau, C.; Di Primo, C.; Lange, R.; Tourbez, H.; Lavalette, D. *Biochemistry* **1997**, *36*, 10262.

(39) Laverman, L. E.; Ford, P. C. *J. Am. Chem. Soc.* **2001**, *123*, 11614.

(40) Hoshino, M.; Kogure, M. *J. Phys. Chem.* **1989**, 5478.